T.R.

GEBZE TECHNICAL UNIVERSITY

GRADUATE SCHOOL OF NATURAL AND APPLIED SCIENCES

A PRODUCTION SYSTEM INVESTIGATION ON NANOMANUFACTURED SENSORS: DIRECT TRANSFER MANUFACTURING OF FLEXIBLE SiC NW-NET UVPDs

MUHAMMED ŞAMİL ÖNDER

A THESIS SUBMITTED FOR THE DEGREE OF

MASTER OF SCIENCE

DEPARTMENT OF INDUSTRIAL ENGINEERING

GEBZE

2022

T.R.
GEBZE TECHNICAL UNIVERSITY
GRADUATE SCHOOL OF NATURAL AND APPLIED SCIENCES

A PRODUCTION SYSTEM INVESTIGATION ON NANOMANUFACTURED SENSORS: DIRECT TRANSFER MANUFACTURING OF FLEXIBLE SiC NW-NET UVPDs

MUHAMMED ŞAMİL ÖNDER
A THESIS SUBMITTED FOR THE DEGREE OF MASTER OF SCIENCE
DEPARTMENT OF INDUSTRIAL ENGINEERING

THESIS SUPERVISOR
PROF. DR. AYHAN DEMIRIZ

GEBZE
2022

T.C.
GEBZE TEKNİK ÜNİVERSİTESİ
FEN BİLİMLERİ ENSTİTÜSÜ

NANO-İMALAT SENSÖRLER ÜZERİNE BİR ÜRETİM SİSTEMLERİ SORUŞTURMASI: ESNEK SiC NANOTEL-AĞ UV FOTODETEKTÖRLERİN DOĞRUDAN TRANSFERLE İMALATI

MUHAMMED ŞAMİL ÖNDER
YÜKSEK LİSANS TEZİ
ENDÜSTRİ MÜHENDİSLİĞİ ANABİLİM DALI

DANIŞMANI
PROF. DR. AYHAN DEMİRİZ

GEBZE
2022

GEBZE TEKNİK ÜNİVERSİTESİ	**YÜKSEK LİSANS JÜRİ ONAY FORMU**

GTÜ Fen Bilimleri Enstitüsü Yönetim Kurulu'nun 20/10/2022 tarih ve 2022/55 sayılı kararıyla oluşturulan jüri tarafından 03/11/2022 tarihinde tez savunma sınavı yapılan MUHAMMED SAMIL ONDER'in tez çalışması ENDUSTRI MUHENDISLIGI Anabilim Dalında YÜKSEK LİSANS tezi olarak kabul edilmiştir.

JÜRİ

ÜYE
(TEZ DANIŞMANI) :PROF.DR.AYHAN DEMIRIZ

ÜYE : DR.OGR.UYESI RECEP ONLER

ÜYE : DR.OGR.UYESI ELIF ELCIN GUNAY

ONAY

Gebze Teknik Üniversitesi Fen Bilimleri Enstitüsü Yönetim Kurulu'nun
...…/…..../……… tarih ve ….…/…..... sayılı kararı.

İMZA/MÜHÜR

SUMMARY

In this thesis, production procedures of nanowire and thin film based uvpd devices are going to be demonstrated with a detailed investigation from the viewpoint of industrial engineers such as; randomness of CVD, PVD, and device production, standardization of cleaning with sonic bath for materials, quality control with SEM, and optical microscopy, design of the experiments and measurements with Keithley, product life cycle analysis by bending tests and their results and innovation steps as a general picture with economic analysis.

Flexible and invisible devices are expected to meet increasing consumer demands for upgrades in wearable devices, smart electronics, and photonics such that retinal prosthesis, e-skin, imaging, and DNA biosensor are just a few of these flexible and foldable devices. In this work, a scalable manufacturing process provides the prototype of wearable ultraviolet photodetector (UVPD) via direct transfer method with silicon carbide nanowire-nanowire junction (SiC NW-NW junction). Rise and recovery times of 1.69 s and 2.24 s exhibit good speed to UV-light without any bias voltage. The comparable current levels are vital in terms of powerless operations and long-lasting energy usage. Indeed, the powerless device generates a photocurrent-to-dark current Ratio (PDCR) of 15 with a responsivity of 5.9 mA/W at 254 nm wavelength. Durability to challenging circumstances of the prototype is tested with sufficient bending cycles. Even after 75 bending cycles, it kept functioning ~96 % of the rest state with respect to current levels and PDCR. The manufacturing process used here eases the burden of nano-manufacturing for large-scale integration, by the mean of providing a method excluding expensive photolithography and pave the way for new design of experiment in diverse wearable optoelectronic products.

Taking everything into consideration, randomness of CVD, PVD, and device production, standardization of cleaning with sonic bath for materials, quality control with SEM, and optical microscopy, design of the experiments and measurements with Keithley, product life cycle analysis by bending tests and innovation with R&D are going to be investigated by a case, production of nanowire and thin film based UVPD devices from the perspective of industrial engineering.

Key Words: Wearable & Flexible Electronic Materials & Manufacturing, Silicon Carbide Nanowire, Photocurrent Characterization, PDCR.

ÖZET

Bu tezde, nanotel ve ince film tabanlı uvpd cihazlarının üretim prosedürleri, endüstri mühendislerinin bakış açısıyla CVD, PVD ve cihaz üretiminin rastgeleliği, malzemeler için sonik banyo ile temizliğin standardizasyonu, SEM ve optik mikroskopi ile kalite kontrol, Keithley ile deney ve ölçümlerin tasarımı, bükülme testleri ve sonuçları ile ürün yaşam döngüsü analizi ve bunların sonuçları ile inovasyon adımları ekonomik analizi genel bir çerçeveyle detaylı bir inceleme olarak gösterilmesi hedeflenmiştir.

Retina protezi, e-cilt, görüntüleme ve DNA biyosensörü bu esnek ve katlanabilir cihazlardan uygulama alanlarının sadece birkaçı olup esnek ve görünmez cihazların giyilebilir cihazlar; akıllı elektronikler ve fotonikteki gelişmelerin artan tüketici taleplerini karşılaması beklenmektedir. Bu çalışmada, ölçeklenebilir bir üretim süreci, silikon karbür nanotel-nanotel yumağı (SiC NW-NW bağlantısı) ile direkt transfer metoduyla giyilebilir ultraviyolet fotodedektör (UVPD) prototipi sağlanmaktadır. 1,69 s ve 2,24 s'lik yükseltgenme ve indirgenme süreleri, herhangi bir sapma voltajı olmaksızın UV ışığına karşı iyi bir hız sergilemektedir. Karşılaştırılabilir literatürde akım seviyeleri, güçsüz operasyonlar ve uzun süreli enerji kullanımı açısından hayati önem taşımaktadır. Gerçekten de, güç olmaksızın çalışan cihaz, 254 nm dalga boyunda 5,9 mA/W'lik bir yanıtla 15'lik bir fotoakım-karanlık akım oranı (PDCR) üretir. Prototipin zorlu koşullara dayanıklılığı, yeterli bükme döngüleriyle test edilmektedir. 75 bükme döngüsünden sonra bile, mevcut seviyelere ve PDCR'ye göre olağan normal durumunun ~%96'sında çalışmaya devam etmiştir. Burada kullanılan üretim süreci, büyük ölçekli seri üretime entegrasyonu için nano-üretim yükünü hafifletir, ucuzdur ve çeşitli giyilebilir optoelektronik ürünlerde yeni deney tasarımlarının yolunu açmaktadır.

Her şey nazar-ı dikkate alındığında, CVD, PVD ve cihaz üretiminin rastgeleliği, malzemeler için sonik banyo ile temizliğin standardizasyonu, SEM ve optik mikroskopi ile kalite kontrol, Keithley ile deney ve ölçümlerin tasarımı, bükme testleri ile ürün yaşam döngüsü analizi ve Ar-Ge ile inovasyon, endüstri mühendisliği ilkeleri perspektifinden nanotel ve ince film bazlı UVPD cihazlarının vaka üretimi ile araştırılmaktadır.

Anahtar Kelimeler: Giyilebilir ve Esnek Elektronik Malzemeler ve İmalat, Silikon Karbür Nanotel, fotoelektriksel özellik, PDCR.

ACKNOWLEDGEMENTS

We, M. Samil Onder and our family, really would like to emphasize our sincere and many thanks to my supervisor, Prof. Dr. Ayhan DEMIRIZ, who inspired me with his profound deep wisdom and converge me through life lessons with his world class liberal way of leadership. His backing, instructions and motivation encouraged me and wish to accomplish every single word in this piece of work.

We owe to highlight our best wishes and special gratitude to Prof. Kaşif TEKER at Advanced Micro and Nano Devices Lab for his co-advisership to our scientific background from freshman year during Undergraduate Teaching Assistantship continued with Graduate Teaching and Research Assistantship to pre-doctoral studies.

We gratitude to Dr. Recep ONLER, PhD and Dr. Elif Elcin GUNAY, PhD for their guidance and being in the jury of this dissertation defense and qualification. Additionally, we thank to Mr. Erdal TOPAC, MS.

I, personally, wish to thank to Zeynep ONDER, my spouse for her life-long friendship, love and eternal support in my hard and dense schedule starting from double major years. I could not forget her devotion and prays to me and my studies, especially her standings with sandwiches ready in break times.

Finally, I wish to express that I have been provided with the real beauty and love of my daughters, M.Elif ONDER, and D.Sumeyye ONDER for their giveth and how feelings they gave me are priceless and beyond description.

TABLE of CONTENTS

LIST OF ABBREVIATIONS AND ACRONYMS

Abbreviation and Acronyms		Explanations
ACE	:	Aceton
Ar	:	Argon
C	:	Celcius
CNT	:	Carbon Nano Tube
°	:	Degree
D.	:	Dimensions
Dia.	:	Diameter
Fig.	:	Figure
GYTE	:	Gebze Yüksek Teknoloji Enstitüsü
HMDS	:	Hexamethyldisilane
H2	:	Hydrogen
IPA	:	Isopropanol (Isopropyl Alcohol)
MOCVD	:	Metal Organic Chemical Vapor Deposition
Ni	:	Nickel
N2	:	Nitrogen
NP	:	Nanoparticle
NR	:	Nanorod
NW	:	Nanowire
NW-net	:	Nanowire Network, Nanowire-nanowire junction
O2	:	Oxygen
PDMS	:	Polydimethylsiloxane
PVC	:	Polyvinylchloride
qtz	:	Quartz
r	:	radius
sccm	:	standard cubic centimeters per minute
T	:	Temperature
TF	:	Thin Film
Ref.	:	Reference

LIST OF FIGURES

LIST OF TABLES

1. INTRODUCTION

A briefing regarding nanotechnology market and semiconductor industry are briefly provided in this chapter. Comparative studies as substitutes are given. In addition, a research background on photocurrent transportations of NW-Net UVPDs and reported indicators are reviewed. This chapter of the dissertation tries to outline better understanding as a general picture and some basic concepts.

1.1. Market & Industry

Nanotechnology and semiconducting electronics have been driven the attention of the last decades due to their role in the manufacturing of quantum computers. Silicon, the material, has named the industry and even the Silicon Valley. Although there is no written strict rule, researchers are unanimously agreed on the definition of the nano-industry, that the materials, under the 100 nm, are considered as nanomaterials. They are often clustered into their dimensions as zero-dimensional (0-D), one-dimensional (1-D), and two-dimensional (2-D) materials. To sum up, 0-D materials, take nanospheres and quantum dots (QDs) for instance, are the ones that none of their dimension in three vector space (abscissa, ordinate, and applicate) are more than 100 nm. Secondly, nanowires (NWs) and nanotubes (NTs) are well-known examples of 1-D materials that just one of their dimensions exceed 100 nm. Moreover, thin-films (TFs) and nanosheets are literally 2-D materials that their width and length are more than 100 nm but not thickness. Among these, NTs are achieved by making the nanosheets as cylinder and NWs are differently synthesized with catalysts in the chamber of a CVD reactor however, these 1-D materials are up-and-coming in consumer electronics owing to physical, electromechanical, and photonic properties [Wang et al., 2014]. They are more likely to be used in ocular eye [Lee et al., 2012], artificial skin [Xu et al., 2018], imaging [Yip et al., 2019], and deoxyribonucleic acid sensing [Demesa et al., 2019] due to their novel characteristics such as sub-atomic size impacts, excessive surfaces per unit volume in nanoscale [Serre et al., 2015]. ZnO [Ouyang et al., 2021, Kumar et al., 2022, and Grottrup et al., 2017], ZnS [Ouyang et al., 2021 and Liang et al., 2012], WO3 [Li et al., 2011], Ge [Aksoy et al.,2012], SnO_2 [Hu et al.,2011], V_2O_5 [Shafique et al.,2019], Si [Serre et al., 2015 and Um et al.,2019], GaN [Teker, 2014], and AlN [Ali and Teker, 2019] have been employed as substitutes. Among these, Silicon Carbide (SiC) is prominent since it is chemically stable, biocompatible, resistant to radioactivity, desirable in terms of stiffness to keep running in extreme circumstances [Lien, 2013]. Now, the benchmark of the candidate materials has been provided due to the vitality of choice of materials and material-forms.

In terms of atomic structure, which affects the properties of materials incredibly in massive forms, 3C-SiC, 4H-SiC, and 6H-SiC are common cubic and hexagonal structural forms of SiC that are accessible and available in the natural world. Typically, the 4H-SiC and 6H-SiC polytypes are referred to as α-SiC, while 3C-SiC is referred to as the β-SiC structure and sphalerite due to its cubic crystal structure. In comparison to hexagonal crystal forms of SiC, Body Centered Cubic (BCC) structure SiC is often preferred because the mass production (in nanoscale) and inexpensive costs in lenient conditions such as atmospheric pressure (P), so that no vacuum needed or affordable temperature levels [Lien, 2013]. This dissertation investigates photocurrent property of a network 3C-SiCNWs based UVPDs with bridging channel width between 33 and 50 microns.

1.2. Reported Studies

In Silicon industry, nanowires forms of SiC have a lot of great characteristics, such as high breakdown voltage, high thermal conductivity, high drift velocity physical and chemical properties, and compatibility. This has made them very popular. Nanowire-network forms of SiC technology can provide significant benefits in terms of temperature (T), power consumption, and operating frequency when compared to limits of recently available Si devices. Until today, most of very few reported studies on optoelectronics of SiCNW UVPDs illustrate close performance in terms of photo-to-dark current ratio (PDCR) and responsivity. Additionally, the early efforts stuck with lack of information about the alignments of nanowires, compatibility of single nanowire device prototype preparation to mass production as economies of scale, and repeatable use of the physical masks that shortcuts the lithography. Moreover, those reports had slower response time based on rise and decay time figures.

The early works on optoelectronics have been investigated through ZnO nanoparticle-nanorod (NP-NR) network device by Ates et al. [2012], ZnO nanoparticle-nanoparticle (NP-NP) network ink on a paper substrate by Kiasari et al. [2014], a single WO_3 NW on a paper substrate by Zhang et al. [2011], a single ZnS NW on a rigid Si/SiO_2 substrate by Liang et al. [2012], Zn_2GeO_4 NW-NW junction on rigid Si/SiO_2 substrate by Liu et al. [2012]. When the study of Zhang et al. considered, a single WO_3 NW on a paper was designed with response time varying from 3 s to 20 s at the voltage of 10. While the device Kiasari et al., ZnO NP-NP network ink on a paper was performing between 3 s and 6 s, ZnO NP-NR network device demonstrated 16 s response time at 2 V in the study of Ates et al. Liang et al. also reported a single ZnS NW on a rigid Si/SiO_2 shows 60 s response time when 10 V applied and Liu et al.'s Zn_2GeO_4 NW-NW junction on rigid Si/SiO_2 device records between 2.5 s and 4 s at 2V. To conclude, this work's device performed better accuracy, precision, and response times at even 0 V, 0.5 V, and 1 V such as 1.690 s, 1.996 s. and 1.955 s respectively.

Nonetheless, most of reports of these devices are produced a III-V (B group elements in periodic table, well known terminology in literature) or a combination of III-V compound semiconductor and on the rigid substrate, which makes the procedure easier; however, it is fragile, incompatible to human anatomy, and underperforming. Thus, SiC-NWs are great substitutes for the manufacturing of reliable and flexible electronics and photonics. Table 1 shows detailed compared reports. In this point, it is crucial to highlight that most of the compared studies reported from much higher bias voltages.

1.3. Dissertation Outline

The top-down and bottom-up approaches are insufficient to chip manufacturing industry so that there is a growing room for additive manufacturing due to the magnificent advancement of the technology. Nano-manufacturing, therefore, has been distinguished from conventional manufacturing in terms of industrial engineering disciplines as scheduling, batch-sizes, and so on. There are certain tests and analysis that have been employed, take the processor companies intel and Ryzen for instance, thereby i3, i5, i7, i9, R3, R5, R7, and R9 processors are based on the normally distributed quality control results. Nevertheless, these tests are conducted after manufacturing stages that beyond the scope of this dissertation.

Table 1.1: Performance comparison of SiCNW-NW UVPD with other reports (Rgd: rigid substrate, Flex: flexible substrate, GO: GrapheneOxide, TF:Thin Film, TT:This thesis).

Material Form	**Volt.**	**Sensi-tivity**	**Rise t (s)**	**Fall t (s)**	**Responsivity (mA/W)**	**Gap (µm)**	**Reference**
Flex Reduced-GO TF	2	-	-	-	4.0	-	[Wang et al., 2014]
Rgd SnO^2-NW	0.01	748	128	400<	$5.5x10^8$	0.4	[Jiang et al., 2017]
Rgd CuSCN-NW	2	720	1.0	50.0	79000	0.15	[Wyatt-Moon et al., 2017]
Flex AlNNW-net	2 &15	~31.6	0.27	0.41	2.43	50	[Ali & Teker, 2019]
Rgd ZnO-NW	5	2320	3.9	2.6	~40	250	[Alsultany et al., 2016]
Flex & Rigid Zn_2GeO_4 NWs	2	1600	2.5	4.0	-	1200	[Liu et al., 2012]
Rgd SiC NW	2	~9.91	3.0	5.0	-	2.2	[Teker, 2016]
Rgd Graphene QDs	5	1200	0.13 5	0.1	4.26×10^{-3}	1000	[Zhang et al., 2015]
Flex TiO_2 NRs	-1	6400	1.4	6.1	10.0	2	[Wang et al., 2011]
Rgd ZnO-NanoNeedles	0.3	31100	22.0	12.0	-	200	[Gedamu et al., 2014]
Rgd Ga_2O_3/SiC-TF	-1.3 & -5	381	25.7	16.6	0.714	0.3	[Qu et al., 2016]
Rgd SiC-TF	5 &10	4900	90	120	46.7	0.8	[Aldalbahi et al., 2016]
Rgd GaN NW	5	~1597	-	-	120	200	[Weng et al., 2011]
Flex TiO_2-NW	10	~900	2.5	10.0	$9x10^4$	~7	[Molina-Mendoza et al., 2016]
Flex ZnONWs/G	1	~162.5	9.5	38.0	400	0.6	[Boruah et al., 2015]
Flex ZnO cloth	4	-	3.2	2.8	-	-	[Liu et al., 2012]
Flex SiCNW-net	0	1498	1.690	2.241	5.9	~33	TT
Flex SiCNW-net	0.5	1555	1.996	2.750	8.2	~33	TT
Flex SiCNW-net	1	1478	1.955	1.650	9.6	~33	TT

This dissertation reports key performance indicators (KPI) of photodetectors as sensitivity, rise time, decay time, responsivity, and PDCR by considering the bias voltage applied and gap width. The flexible SiCNW-NW UVPD device worked at low voltages and had a gap width as narrow as ~ 30 microns, which is considerable if the huge costs of photolithography savings are regarded.

This Master of Science dissertation aims to ease the fabrication of SiCNW-NW UVPDs with altering applied voltages, first eye witnessing the impact of voltages on those KPIs listed above and observing the struggles of the innovation management and R&D team because it is significant for a candidate intellectual property and patent attorney that Turkiye has lack of expert personnel in that niche. Thus, it was very decent and excellent experience to feel the research environment by actively doing research in the laboratory for better understanding of the innovation management processes. Under the shadow of these ultimate and noble cause, the prototype of SiCNW-net UVPD on flexible substrate were manufactured after excessive number of trials with overtime work. In this manner, current vs time, current vs bending cycles, current vs voltage, rise and decay times of one cycle, sensitivity vs voltage, response time vs voltage, responsivity-external quantum efficiency (EQE) - band width (BW) vs voltage were recorded methodically. This dissertation has an outline as the following:

To begin with, a discussion on nanomaterials and their characteristics is introduced in the chapter one. Then, the reports in the literature are reviewed on the basis of the optoelectrical features including their indicators. The chapter ends with how this dissertation are organized.

The explanation of manufacturing procedures of SiCNW-net UVPD between nanowire fabrication and end-product, is comprehensively provided in the chapter two. Moreover, the facilities employed in nanowire characterizations such as optical & electron microscopies, X-Ray Diffraction (XRD), sputter coater, manufacturing procedures such as metal-organic chemical vapor deposition (MOCVD) are more or less given due to the fact that the recipe and yield they include as a commercial, a professional, and an intellectual property. At the end, the explanations of the calculations and the properties of produced UVPD prototype as PDCR, sensitivity, rise and decay times, responsivity, EQE, BW, and so on are provided in the chapter two.

Thirdly, the explanation of the photocurrent properties of the prototype has been given in the chapter three. Additionally, the descriptions of the design of experiment and facilities used for measuring have been provided. Furthermore, basic key indicators grasped and the presentation of the recorded figures of the manufactured prototype are given. In addition, the detailed successful outputs with the literature reports have been compared.

Finally, the resulted finding outputs are summarized with contemporary definitions and bottlenecks including the field of intellectual property rights. Next, the discussion on upcoming potential of SiC studies in the form of nanowire and opto-electronical appliances are given in the chapter four.

2.SiC NW PRODUCTION & UVPD PROTOTYPE MANUFACTURING

The detailed explanations regarding manufacturing procedure of SiC NW-net UVPDs between nanowire production and finished good have been provided in this chapter. Moreover, the metrology tools utilized in the characterization analysis of these synthesized nanowires as scanning electron microscopy (SEM), XRD and a brief introduction how nanowires are grown has been described. At the end, the explanations of the calculations and the properties of produced UVPD prototype as PDCR, sensitivity, rise and decay times, responsivity, EQE, BW, and so on are also provided.

2.1. Nanowire Synthesis

Although there are top-down and hybrid approaches, the bottom-up approach is the common mean of manufacturing process for 1-D nanomaterials. That method has two diverse ways, namely, grow-and-place (assembly-based) and grow-in-place (assembly-free). In grow-and-place method, nanowires are fabricated first and then, they are aligned by surface-patterning, magnetic-field/ dielectrophoretic exposing, mechanical printing, and shear forces applying. Langmuir-Blodget, Blown-bubble, fluid-flow directed, stirring-assisted, spray-coater routing, evaporation induced, and strain-release are easily accessible in the literature as shear force-based approaches. Each proceeding has pros and cons regarding complexity, cost of fabrication, and agility for 1-D nanomaterial fabrication.

On the one hand, dry etching, wet etching, and various lithography techniques including photolithography are some of the top-down approaches in the transformation from the bulk form to nanomaterial. In order to get extremely sophisticated control and integration of the patterns are followed in top-down method. Take the photolithography for instance, it has ten-detailed high-tech stages to carry. Think about any small omission, it might result in being trash of all the manufacturing run. Microelectronic and Microelectromechanical Systems

(MEMS) can be employed fine as the products of these top-down methodologies. The cost of the production and eccentricity gets unaffordable to operate further when the materials get miniscule and nanoscale. Therefore, there is a need to seek innovative manufacturing processes to decrease the costs as economies of scale in the chip market.

The synthesis of nanowire forms with top-down method requires excessive control in assorted sizes and patterns like perpendicular or horizontal. Although there are successful manufacturing Si NW applications, they are very sophisticated and have pricey processes, as well as the produced nanowires do not yield that much high. Overall, the disadvantages of these methods in top-down overweigh their advantages.

On the other hand, individual nanomaterial units are assembled in the bottom-up approach for more solid structural materials. Nano-manufacturing is processed in the atomic level, and often atom-by-atom. Therefore, top-down methods like lithography or etching do not have that much precision and include impurities. An advance answer to this technical voidness might be given by the Direct Transfer Method/Manufacturing (DTM). The geometrical constituent with size that open the doors for innovative designations and make the innovations happen by this structural but functional nuances are made by adaptability and grip-providing DTM. Thus, DTM can contribute the betterment of the bottom-up methods in order to integrate the prototypes into the mass production.

Indeed, impurities in the surfaces, alignment of nanowire during and after the synthesis, and type of doping (n-type and p-type) composes the small, remained room as issues and challenges in nano-manufacturing. Beside these, bottom-up approaches are the best-fitted manufacturing techniques by synthesizing the nanowire form materials. Among the variety of the bottom-up approaches, the key-points and versions of Vapor Solid are going to investigated in the following sections.

2.2. Synthesizing Silicon Carbide Nanowires

Numerous ways of the Silicon Carbide nanowire synthesis have been developing day by day. Chemical Vapor Deposition (CVD) is one of well-known methods in these ways and it comprehends Epitaxial Growth in Vapor Phase, chemical reaction, atmospheric pressure (AP) CVD, ultra-high vacuum CVD, and then Sputter coater as Physical Vapor Deposition (PVD) can be supplementarily used (see Figure 2.1).

Figure 2.1: A typical PVD for carbon and gold coating in nano-manufacturing.

To start with, CVD, and PVD might be employed as the methods for the growth. During these methods, some precursor gases are utilized such as methyl trichlorosilane (MTCS), Methane, Propane, Silane, Diethyl silane (DES), Hexamethyldisilane (HMDS), and so on. In the beginning, a composition of Silicon and Silicon dioxide with methane, or a composition of Silicon and Carbon, or Silicon Carbide powder form can be used. In the chamber of the reactor, (100) or (111) Silicon wafers are generally used as base. The reaction-rate or gas-flow mechanisms are two major regimes and the operating environment of the chamber of the CVD is between 1000 and 1400 ˚C. The chemical process can be catalyzed by the nanoparticles of nickel, gold, platinum, palladium, and so on.

In the case of this dissertation, a Metal Organic Chemical Vapor Deposition (MOCVD) reactor is used to synthesize nanowire forms of Silicon Carbide. In order to ensure the deport of all contaminants away, a couple of purges at low pressure is provided inside the chamber. Then, a wafer piece with full of catalyst nanoparticles is placed in-situ/chamber made of graphite (G), called susceptor. After loading the system, source material is provided by virtue of a carrier gas into the in-situ/chamber that is the heart of the fabrication. Depending on the pace of the gas provided on the chamber, reaction-rate limited regime or gas-flow mechanisms affect the structure of the material produced.

Next, the temperature for nanowire fabrication is set by the RF-induction as appropriate level. Then, the surface of the wafer piece is consecutively deposited and chemically reacted varying from a couple of minutes to many hours depending on the reactor (see Figure 2.2). At the end of the fabrication, high-quality nanowires were acquired.

The fabrication run was realized in a horizontally Radio-Frequency induction furnace and HMDS was used as precursor gas. The substrates can be tilted or placed vertically to avoid impurities due to the fact that the difference between inlet and outlet of the gases' access to the reacting material. The nanowires grew on Silicon wafer with 300 nm thick oxidation coating with Nickel nanoparticles that radius of 15 nm for catalyzation purposes. To decontaminate the surface of Silicon wafer (often, from the human-induced anatomical cuticle dirt), a cleaning procedure is followed with a three-stage solvent (ACE, IPA, distilled H_2O) bath and one step gas (nitrogen) compression to remove the solvents. The prepared and the separated each solvent were applied on beaker-glasses. Firstly, the Silicon substrate piece in ACE bath with a jeweler ultrasonic bath during at least 4 minutes. After the ACE bath completion, the wafer piece was sunk in the beaker-glass with IPA at least 3 minutes. Later, the substrate piece was soaked in distilled water. ACE cleans the organic contaminants and etches the polymers thus, it is vital to note that the cleaning procedure for polymer substrates in lab environment is applied as a two-stage solvent (only IPA and distilled H_2O, not ACE). Additionally, masks have a crucial role that surface of the substrate can be easily damaged or contaminated by the exhaling. After the three-stage bath in sonication, a nitrogen was applied with an air compressor to dry remained liquids and chemical materials. The substrate is immediately taken to a covered petri plate to transfer from cleaning room to manufacturing room. The deposition of the nanowires in IPA on prepared substrate such that oxidized SiO_2/Si wafer piece with 300nm oxidation thickness, was applied after the cleaning procedures. Before loading the quartz (qtz) tube which Silicon substrate was situated in-situ of susceptor made of G, the Silicon Carbide Nanowires in the IPA liquid are dried. A 0.05 Torr evacuation was applied to the system before the reaction, and then three consecutive purges for contaminant removal purposes to qtz tube (see Figure 2.3).

Figure 2.2: A model CVD reactor room for advanced manufacturing.

Afterwards, the temperature of the equipment was set to just above 1050˚C by sustaining Hydrogen (H_2) gas at a flow rate of 100 standard cubic cm/minute and Argon (Ar) gas as 100:500 of H_2:Ar ratio so that 500 standard cubic centimeters per minute (sccm) for 5 min. When the conditions reach a balance with stable T, the nanowire fabrication is launched. Throughout the chemical process, T levels were kept at 1100˚C during 15 min while adding Hexamethyldisilane (HMDS) sourcing gas through H_2 carrier gas as 10 sccm at same degree T at 200 sccm rate H_2 with 500 sccm Ar gas flow. The measurement of the P during the process was observed as a sea level. The system has quenched to just below 305˚C, T level via H_2 at a flow rate of 100 sccm and Ar at a rate of 200 sccm before finalizing the run. To sum up, purge, heating, growth/fabrication, cooling, and unloading are the five main steps in the process. Three purges and the evacuation to 0.05 Torr are applied at the stage of purge. This stage takes 15-20 min at T_{room}. In the stage of heating, T reaches just above 1050˚C with H_2: Ar ratio of 100:500 sccm. After the heating, HMDS: H_2: Ar ratio of 10:200:500 sccm at 1 atmospheric pressure continuously provided with stable levels between 20th min and 35th min. Before unloading, the system is cooled with H_2: Ar 100:200 sccm from 35th min to 50th min. The system unload takes less than 10 min.

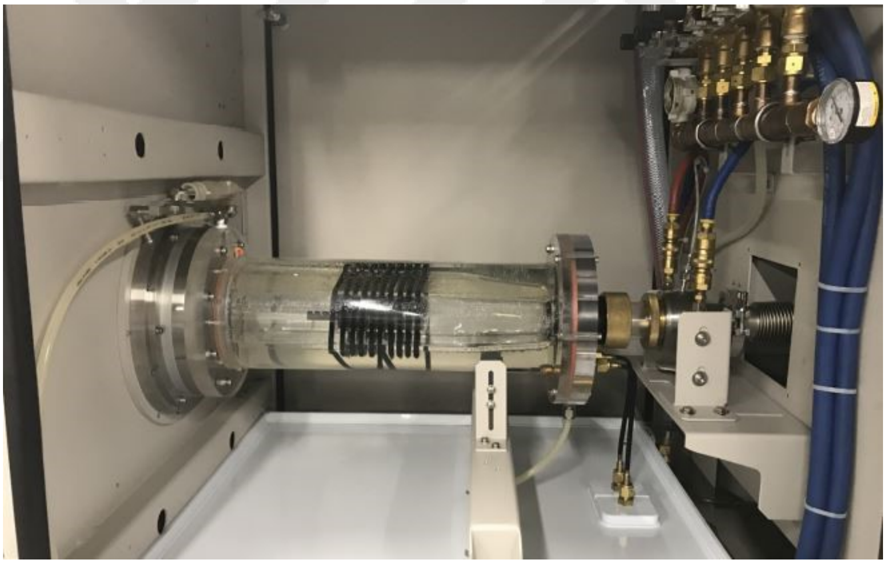

Figure 2.3: Chemical reaction chamber using RF induction furnace in order to reach desired temperatures for nanomanufacturing.

2.3. Characteristics of Silicon Carbide Nanowires

Scanning Electron Microscopy and X-Ray Diffraction are employed to characterize the nano-manufactured wires. X-Ray Diffraction Analysis has been conducted to have the information whether the fabricated nanowires are cubic or hexagonal crystal structure. Scanning electron microscopy has enabled to observe the formation of the surface. The discussion of generated outcomes and the principles regarding how these machineries work hold in the upcoming part below.

Surface morphology of a conducting sample by a microscopy, which uses concentrated electron beaming gun, gathering the back-scattered and secondary electrons (é) by detectors, and scanning the surface by these detected electrons, is called Scanning Electron Microscopy. It can be obviously said that if the surface morphology of the specimen is the issue, scanning electron microscopy is one of the first choices due to ease of use. Much higher resolutions and better in quality photographs can be captured when compared to standard microscopies using basic lenses. In addition to the beam of electrons, some advanced and vacuumed condenser lenses that electromagnetically worked, usually composes the key components of the scanning electron microscope. Electron gun collects electrons and upgrade them into required energy levels with desired acceleration from 1000 eV to 40000 eV in the microscopy. Next, the condenser lenses create a focal point probe by virtue of these upgraded és on the sample in the chamber of the microscopy. The two detectors generate the és primarily and secondarily after hitting the specimen and reflection so that the display of the microscopy has the data of scanned surface area to show after the analysis and merge of the és. It is crucial to note that back-scattered detector collects the primary electrons to return a display regarding topology and morphology of the surface while secondary electron provide the magnified data by detecting secondary electrons, which have low energy levels. Overall, the image processing collected data is illustrated by the monitor screen. To summarize a standard scanning electron microscope (SEM) workflow, the electron gun at the top of the microscope provides electrons to electron beam, then they are condensed by an advanced lens. Afterwards, they pass through coils of scan to control the magnification. Next, objective lens is used to focus the electrons through the specimen, perfectly elastic collided electrons detected by back-scattered detector and inelastic collided electrons with low energy collected by secondary electron detector to amplify. Therefore, the image on the monitor is composed by merging the data from these two detectors (see Figure 2.4).

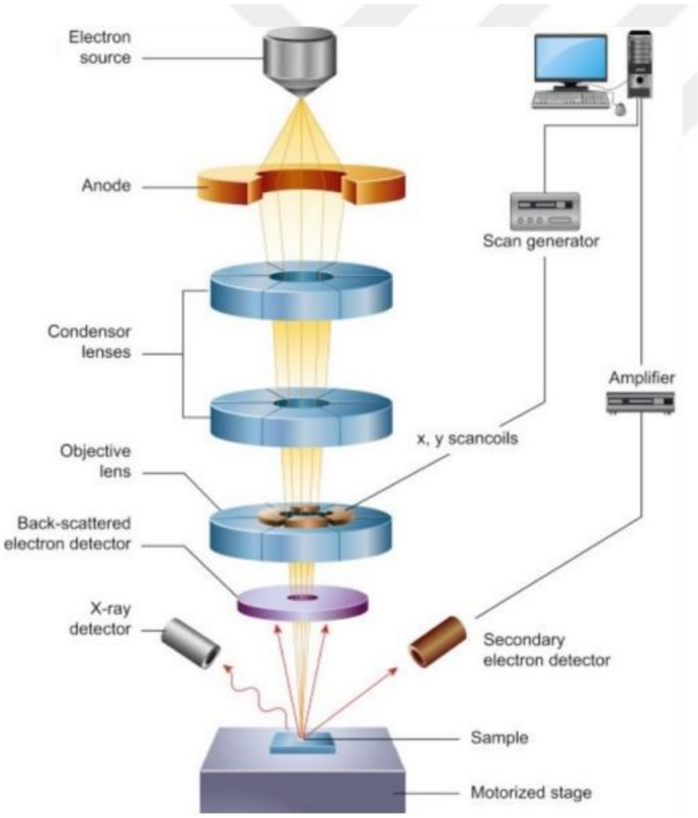

Figure 2.4 The mechanism of the scanning electron microscopy

A Phenom XL desktop SEM is utilized in the Advanced Micro- and Nano-Devices Lab, Marmara University for this dissertation. The photographs are taken at magnification levels between 80x and 1000x and at resolutions as small as 10 nm owing to the SEM.

Silicon Carbide Nanowires fabricated using Nickel NP catalysts on a Silicon wafer piece with a 300 nm thick oxidized layer, are photographed a couple of times by scanning electron microscope. A variety of captures in magnified up to 10000 could have been taken. The distribution of Silicon Carbide nanowires on the Silicon surface as clew and varying density levels with the radius between 20 nm and 35 nm are clearly seen in these captures. The nanowires differ from 1-2 microns to 20-30 microns-long (see Figure 2.5.a).

Secondly, an unlethal technique that the atomic bindings of matters are investigated by x-ray analysis, is called X-ray diffraction (XRD). XRD illustrates the crystal structure in order, morphological features and inter and intra molecular bindings on the data of analysis using some methods and parameters such as how much degree angle scattered, how much the material polarized, how long the wave is, how much energy the atomic beam diffracted by specimen. The principle of a regular XRD is as follows: A source provides x-ray waves by optics. A two-dimensional detector collects the data from x-rays and computes their scattering angles. Finally, a goniometer displays the video for x-ray applied and aligned specimen.

In the results, it might be easily said that there are Silicon Carbide Nanowires based on the XRD conduct of analysis and evaluations. (see Figure 2.6). The angle of the diffracted rays is shown in apsis with two maximums around ~36˚ and ~60˚, so that represents BCC structure and the plane of (220) in order. It can be implied that the BCC form of Silicon Carbide is the dominant crystal structure based on the XRD analysis.

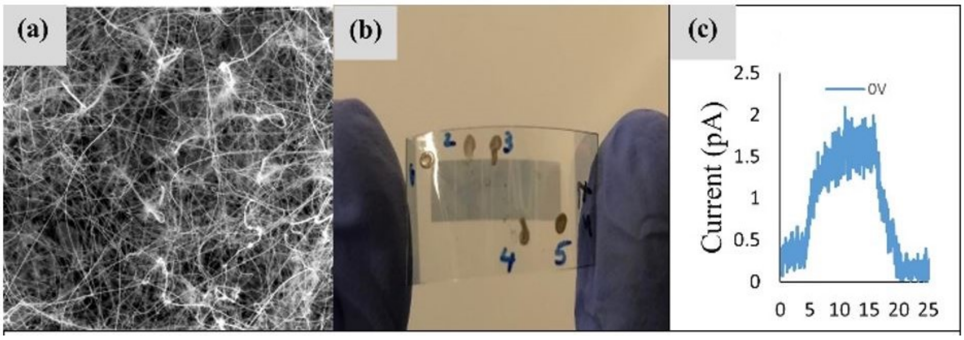

Figure 2.5: a) Produced dense nanowires on SEM. b) The picture of the produced device bent intentionally to show the flexibility c) The I – t data recorded at 0 V.

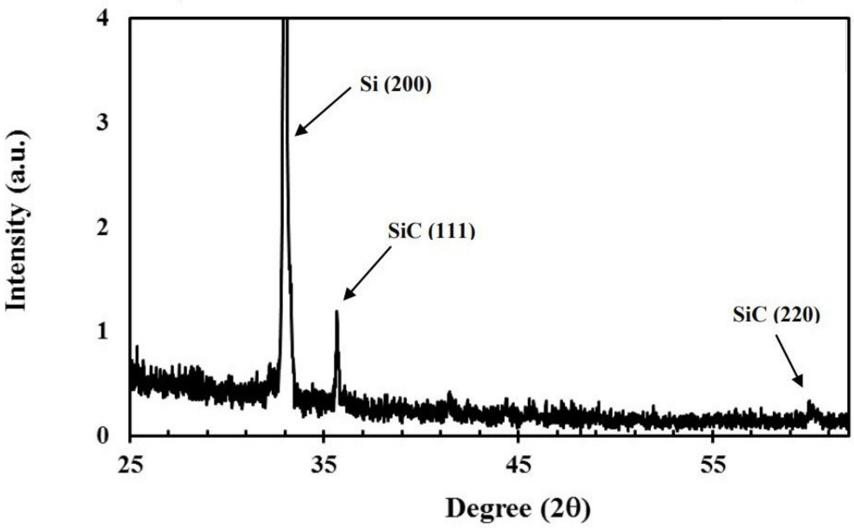

Figure 2.6: The X-ray Diffraction results.

2.4. Flexible SiCNWNW network UVPD, Prototyping, and Quality Control

The upward trends in consumer (see Figure 2.7) products in wearables, smart devices, and optoelectronics tend to be met by foldable and non-opaque devices [Wang et al., 2014]. Compared to substitute semiconductors, super features inside Silicon Carbide as nanowire state since it is inert, resistant to radiation, hard, ductile, stable, durable in difficult circumstances, and so on [Lien et al., 2013]. Moreover, nanowire based UVPDs are able to work powerless and reduce the manufacturing costs by surrogating overpriced and relatively uncontrollable lithography technique with economical and facile physically masked DTM. Furthermore, nanowire based UVPDs are compatible with flexible substrates to be applied as Silicon/Semiconductor On Insulator (SOI) as well as Metal Semiconductor Metal (MSM) forms, which are generally rigid wafer substrates in chip-industry. Instead of thin film (TF) or bulk form, nanowire based UVPDs are photo sensors which use nanowire-network tangle or a sole nanowire as the matter between the electrodes. Under normal circumstances, Drain(D), Source(S), and Gate(G) composes the nanowire-based sensors; however, D and S are two terminals used in the work, also known as back-gate. Nanowire-nanowire networks and junctions without Au-electrodes are actively open to targeted UV exposure. That is the reason why it is maximized detecting interactions in back-gate nanowire-network based UVPDs. In other words, there is a trade-off from the controllability to facile and decreased-cost nanomanufacturing. Therefore, there is no need to control the current of the sensor in the low bias voltages, so that the ultimate control is not necessary. In addition to this, high-priced and complex nanomanufacturing with strict procedures are by-passed. All in all, rigid silicon wafers can be employed for the purpose of back-gate nanowire based UVPDs as MSM. Despite the fact that silicon wafers are rigid and unable to fold, some of the flexible polymers like Polydimethylsiloxane (PDMS) are seen for SOI devices in the studies on the doctrine. Nevertheless, PDMS needs an extra curing agent and adds another time and procedure to the total time of manufacturing. Thus, Polyvinyl chloride (PVC) is one of the best fit and applicable products of massive production, very inexpensive as economies of scale, and easily accessible in 1 Dollar stores.

Silicon Carbide Nanowire-Network UVPDs are produced on insulator PVC in this work, and optoelectrical property is recorded as voltage applied between the source and drain electrodes.

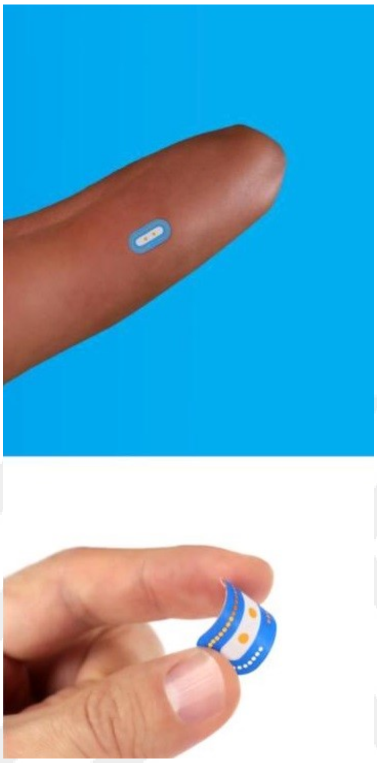

Figure 2.7: Wearable Electronics, a sample use of flexible UV sensor.

DTM method is utilized for nanomanufacturing the prototype of flexible Silicon Carbide Nanowire-Network UV photosensor in the dissertation. Then, the KPIs such as PDCR, responsivity, rise time, decay time, sensitivity figures were computed and reported with respect to the gap-width as roughly 33 microns. A couple of trial-error was enough to pass learning curve and prototype a working end-product.

To manufacture the foldable product, nanowire tangles made of Silicon Carbide in IPA solvent as a suspension, were sonicated at least 2 hours for the purpose of alignment of nanowires before dispersing on the foldable basis. Simultaneously, the previously explained cleaning procedure is applied before dispersing the drops on the preparing substrate except acetone (ACE) since, it etches the polymers/plastics (see in Section 2 of Chapter 2, page 9) to remove the contamination. It is because the main source of contaminants are people and even a careless exhale affect definitely to the quality of the device in production if upscale cleanroom is avoided as in our case. Further, an IPA-NW suspension is taken with disposable serological micropipette as small as 10 µL in order to drop on 1 cm x 3 cm piece of substrate four times with equally likely distances in order to increase the chance of fabricating working device by DTM. The thickness of the basis was measured as just above 1600 microns with a caliper. A couple of physical masks have been cut, namely Silver, Brass, Stainless-steel by jewelry and PCB laser cut subcontractors as contract work. The stainless-steel mask designed and prepared by BEK Laser in YEDPA had the best of our trials in terms of better contacting section. Due to the fact that sputter coater has bridging deposited Au layer so that the device does not work, the contact is crucial for this manner. Thus, a contact as flat as possible is required because the laser cutters generally lead to melting of the physical masks. Therefore, there is a great possibility to have surface impurities of the corresponding face of the mask's melted sections to the substrates, which is not desired and need to avoid. To have a such a physical mask is one of the extremely vital points of this work since it substitutes the expensive and complicated photolithography. Beside there are very few studies about Silicon Carbide nanowire fabrics UV photosensors on flexible substrates at much more voltages applied, another key and outstanding milestone is that there is no report on a powerless Silicon Carbide nanowires-network/tangle UVPD sensor with an inter-electrode channel width of ~30 microns at 0 V as of today.

Now, the prepared physical mask, the contaminant-free substrate, and an array of nanowires as much cured and aligned as possible are ready to fabricate the device. In this point, it is significant that the micron-level thick sections of the corresponding flat surface of the mask blocks the Au coating in physical vapor deposition (PVD). According to Wadsworth et al. quality control is how fit the device to the usage intension is [1986]. Up to now, the quality control and formations of the nanowires produced in MOCVD has been tested by XRD and SEM first (see Figure 2.8).

Figure 2.8: Our SEM in Gebze Technical University with EDX.

Secondly, the quality control of the contacting section of the physical mask has been tested, determined, and marked. It is time to place the mask extremely carefully covering the nanowire-network/tangle dropped areas to have a quality device. This quality control can be provided by a simple optical microscope owing to the allowance of the nanowire-batch size, so some of these total masses in our research and development (R&D) process are even distinguished by the naked eye. After placement of the mask, magnets are employed to stabilize the mask on the nanowires-dropped substrate. Therefore, a sandwich-like materials, magnets at the bottom, insulator polymer, nanowires, and stainless-steel mask at the top are ready to gentle placement inside the dismountable and mountable PVD chamber on the stubs. Finally, the Au electrodes has been deposited by PVD. Now, the device is fabricated; nonetheless, the fourth quality control test is done by SEM, or optical microscope. It can be obviously said that SEM (PhenomXL) is relatively expensive to buy than an optical microscope, the operator requires more pricey education to take and more wage to hire, SEM needs the filament component to be replaced every 15-20 months period likewise the toner of the printers, the equipment of super-computer including vacuum-pump consume much more energy to operate. In this forth quality control, the device is checked whether there is a union of the Au pads quickly. The latter quality control is realized by applying current and voltages to these electrodes as the fifth quality control test in the Keithley (2634B) source meter under probing while measuring the active nanowire-network active area (it is exposed to UV in order to compute the performance parameters of the device, this area is taken roughly as trapezoid or quadrilateral thin-film for the sake of simplicity). Sixth quality control is the repetition of the fifth quality control after bending tests by manual work with 90° done likely in the literature to forecast approximate product life cycle (PLC). The performance of nanomanufactured device that ensured working well is recorded by illuminating 1.8 mW per cm^2 intense (13.5 Watt per meter squared area) ultraviolet with the wavelength of 256nm under the circumstances; T_{room}, 1 atm, after sunset (~ midnights), remote and semi-autonomous by Arduino, the probe station covered with $1m^3$ cardboard box if during the day measurements are necessary, which provide dark environment so as pure as only the UV trigger the device as power source and blocks any micro and nano scale interference. Remote controlling and box coverage is used for avoiding any intervention even the movements of the air molecules, or vibration of the laboratory workbench or walls adjacent to the lab bench. It is clearly observed that when a tractor passes by the lab building or there is a noise of a group of people outside the lab wall, the measurements are affected negatively. Taking everything into consideration, the recordings are usually taken during the midnights. Arduino is used to apply a micro-level robotic process automation (RPA), nevertheless it might be seen as semi-autonomous since the starting and ending the measurement are decided by researchers and only consecutive turning ON and turning OFF of the UV lamp every 10 seconds are done automatically.

3. SILICON CARBIDE OPTOELECTRONIC CHARACTERIZATION

Design of the Experiments to measure optoelectronic property of BCC Silicon Carbide Nanowire-form material and results of former reports with the latter are presented after introducing the key performance indicators namely, PDCR, Sensitivity, some of the indicators after the harsh use simulation of bending tests, Responsivity, Rise, and Recovery Times in the section below. These demonstrate why I – t measurements have a crucial role. Further, the nano-manufactured NW-net UV sensors are mentioned with the discussion about compared indicators. All in all, the context of generated data on a probe station with a Keithley 2634B source-meter is comprehended as the broader frame so that meaningful information facilitated to develop knowledge to give an insight.

3.1. Description of KPIs

Various figure of merit KPIs, particularly, PDCR, Sensitivity, I – t measurements with light on-off consecutive cycles, bending test to simulate Product Life Cycle, Responsivity, Rise, and Decay Times might facilitate to interpret the optoelectrical characterization of SiCNW-net UVPDs. The brief descriptions including the measurements of the nanomanufactured prototype are introduced in this part. The results of the indicators build up hopes and are promising, therefore there are still room for photonic characteristic improvements of industrial electronics.

3.1.1. PDCR and Sensitivity

Photo-to-dark current ratio (PDCR) is the ration of current on the figure, OFF-state subtracted from the ON-state over OFF-state of a UVPD device $(I_{ON} - I_{OFF})/I_{OFF}$. Having said that the degree of blockade the photocurrent flow in OFF-state is shown by the PDCR of the photodetector. Replacing the pricey photolithography in fabrication is vital since it rises the total cost of the production and requires extra rigorous experts to block the variation in quality as well as the lost wastage in the production. To sum up, the machinery is expensive, the procedure is complex and can cause undesirable bad variations as poor-quality products, the technical personnel should be accurate and precise, the training and education of these personnel takes time and money. In this point, laser-cut stainless steel physical mask is the shortcut of whole these massive expenditures and it is re-usable. However, it is important to note that expecting an extreme PDCR figure by Nanowire-form UVPD is not that much easy comparing to traditional transistors and sensors as NW-form devices might not pass to OFF-state very fast. Secondly, the sensitivity is another highly common indicator for characterization in the literature that illustrates how well the detector sense the light and it is unitless as well as PDCR. Sensitivity (S) is usually accepted as the hundred times PDCR [AlZoubi et al., 2018].

3.1.2. Responsivity, Rise, and Recovery Times

OFF-state subtracted from the ON-state is calculated first for the Responsivity (R). Secondly, light exposed active area (A) is multiplied with the intensity of UV lamp's power (p). Next, the first result of the calculation is divided into the second number of multiplication result for R, as $R=[I_{ON}-I_{OFF}]/(p \times A)$. Therefore, the unit is appeared as $A \times W^{-1}$ [Xu et al., 2018 and Kiasari et al., 2014]. Moreover, the rise time is recorded as the corresponding value where the current has 90% after the light turned on. In order to calculate the value, the subtraction the ON-state minus OFF-state, is multiplied by 10% and then, the result of this multiplication is subtracted from the current the ON-state at steady state $\{ I_{90\%}=I_{ON(Steady)} - (0.1) \times [I_{ON}-I_{OFF}]\}$. It is important to note that the unit of the calculation is in Ampere (A) and t_{rise} is the corresponding value of this photocurrent value on the time showing x-axis. Furthermore, the recovery time is calculated as the 10% after the light turned off. To compute the value, the subtraction the ON-state minus OFF-state, is multiplied by 10% and then, the result of this multiplication is added to the OFF-current at steady state $\{ I_{10\%}=I_{OFF(Steady)} + (0.1) \times [I_{ON}-I_{OFF}]\}$. Thus, the corresponding value of this current on the time-axis is the $t_{recovery}$.

3.1.3. The Photocurrent – Time (I–t) Results and Optoelectrical Characteristics

Record of the current – time (I – t) measurement is taken before the bending tests at 0 V, 0.5 V, and 1 V during 2 minutes with 10 seconds pulses for showing off of merits of the SiCNW-net UV sensors as in Figure 3.1. Beside other low bias voltages applied, the zero bias is intentionally recorded to validate and verify if the prototype might operate self-powered. It can be obviously said that the sensor illustrates a 15-times rise current level in 254 nanometer-long wavelength ultraviolet exposure with no power source needed. The current – time measurement records are taken at as low as 0.5 V and 1 V biases to evaluate the performing behavior of the sensor after proving the self-powered work of the sensor as depicted in Figure 3.1.

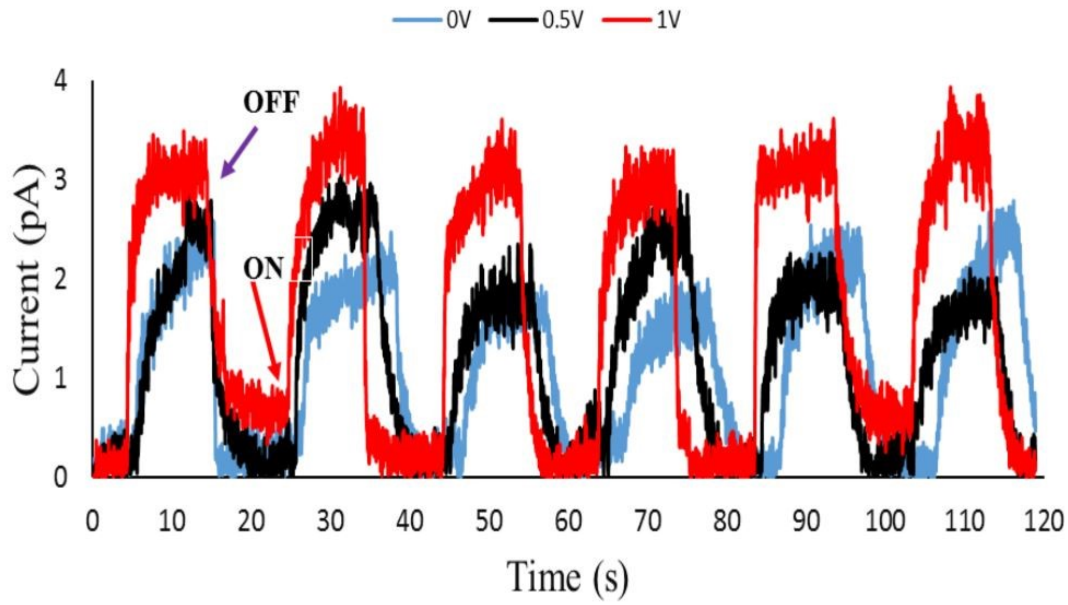

Figure 3.1: The I – t figure at different low voltage biases.

It is significant to conclude that the generated photocurrent under the ultraviolet light is directly proportional to the bias voltages. Furthermore, the off-state current level is 140 fA on average, where the on-state current level is ~150 fA for zero bias, 240 fA for a half volt bias, and 300 fA for one volt. The cycles of the sensor to the ultraviolet illumination demonstrate the applicability of our sensor among various photonic electronics with the absence of power source such as a battery. The results at 0 V unveils a powerless characteristic feature of our Silicon

Carbide nanowire tangles UV sensor. Indeed, it can be said that the sensor is vertically SOI, and horizontally MSM device. It is not expected that regular MSM devices reveal any current under light exposure at 0 V. The NW-NW junctions are the reason why there is a current under the UV light. In addition to two inter-electrode channel between the gold electrodes and the distinction Silicon Carbide NW-NW junction, an extraordinary MSM device is built. The large gold pad exposed areas are depleted between the gold and Silicon Carbide NW-tangle junction resulting in Schottky barriers inter-contact areas. The potential difference in these structures develop an embedded inherent current causing the current under the light at 0 V [Goswami, 2020].

3.1.4. Reliability and Product Life Cycle Simulation

Roughly 90˚ bent device from the steady-state are applied to the tests similar to the studies in the literature for the purpose of simulating the final product's reliability and product life. The bent device is released to have the rest of its steady-state, and this loop is conducted 10 times, 50 times, and 75 times back-to-back. In fact, much satisfactory stable and repeatable performance is observed and is displayed by the indicators of the sensor under extremely many times bent sensor (see Figure 3.2).

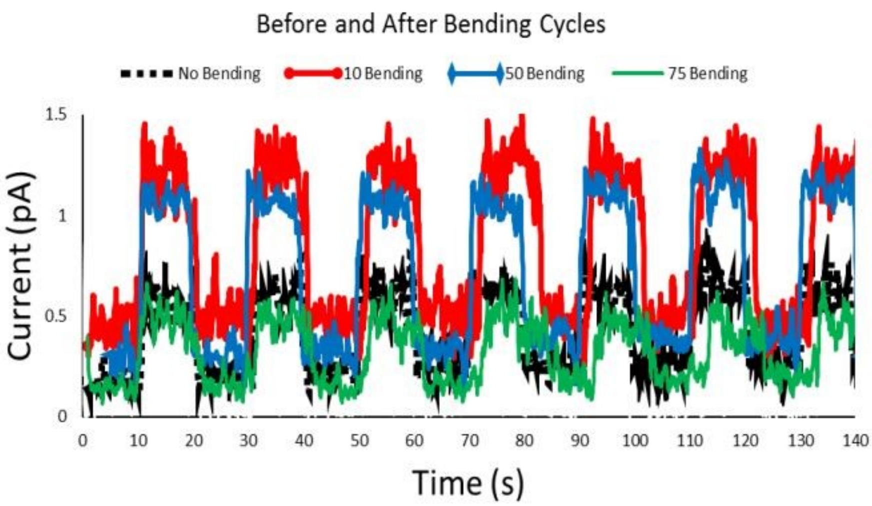

Figure 3.2: The I – t figure of pre and post bending tests.

Comparing with the initial-state indicators, the prototype's Photo-to-Dark-Current-Ratio is very satisfactory with the 95% of that figure even after 75 harsh bendings. It can be clearly inferred that the PLC of wearable electronics and optoelectrical detectors are parallel to the Silicon Carbide nanowire tangle/network UV sensor's product life fabricated and reported in this work.

3.2. Design of Experimental Set

In the section of Synthesizing Silicon Carbide Nanowires, the recipe of the MOCVD procedure had been introduced in-detail. The morphology of the nanostructure is monitored utilizing SEM after the chemical synthesis. The Silicon Carbide nanowires have a high length-to-diameter ratio owing to the length, even as long as 100 microns. In order to inspect the crystal structure of the Silicon Carbide NW-form, XRD facilitates our work to analyze it.

Next step is that Silicon Carbide NW network/tangle are taken into IPA solvent as a suspension to manufacture the device. Silicon Carbide NW network/tangles in IPA are released on the PVC substrate (1 cm x 3 cm x 0.17 cm) by DTM. Remember the solution of the IPA-NW mix is sonicated during the 120 minutes and the PVC substrate is cleaned with followed two-stage procedure. The previously explained readily prepared physical mask with the pattern of five gaps and four wires is employed to have Au pads by PVD. The mask substitutes the photolithography and etching for reducing the cost, time, and variation of the nanomanufacturing. The UVPD has interelectrode space as~30 microns, whereas the wires of the mask are as

Figure 3.3 – A source meter used to record I – t and I – V measurements.

thick as 50 microns thanks to the deposition mechanism of the sputter coater, PVD. UVGL-58 UV source near to the probing equipment and Keithley (see Figure 3.3)

(2634B) source meter is used for measuring the optoelectrical data at dark environment and T_{room}. The nanofabricated flexi-UVPD prototype is put to test on 13.5 W/m^2 intense power, 254 nanometer-long wavelength UV exposure, and at d=4 cm, where d is the distance between the UV and the UVPD. The UVPD is gently placed on the station of probing (see Figure 3.4). An embedded vacuum pump is employed to keep the UVPD stable at the rest-state and to prevent electrodes from any potential hazards. Then, each probing tip is aligned and located by the help of optic microscope.

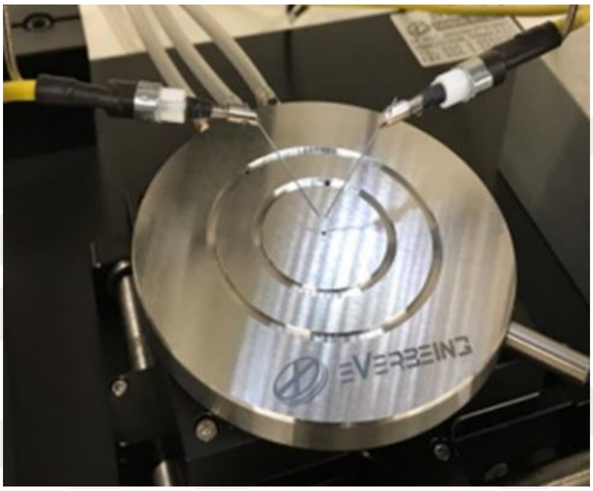

Figure 3.4 – The probe station and needles used by probing the UVPD device

The photocurrent versus time (I – t) data is recorded. The intervals of turning the light on and turning off is 10s. The Labview SW is employed by an Arduino-kit like a remote-controller as previously explained in-detail. The testing environment and dark room conditions are defined in the former chapters as well. Bendings are applied as the simulation of re-usability and forecasting the product life for PLC analysis.

Silicon Carbide nanowires have radius varying from 15 nanometer to 35 nanometer. The length of a nanowire is approximately 20 microns on average. XRD analysis is accomplished by the wavelength of 0.154 nanometer Cu – K_α for assessing the crystal structure of Silicon Carbide NW-form. Zinc blende structure is observed by XRD graph. Furthermore, figures of SiC[200], SiC [111], SiC[220] are obviously seen with local peaks and global maximum.

Characterized Silicon Carbide NW network/tangles are then, used to manufacture flexi-UVPD sensors. The photograph of pre-patterned steel mask for sensor electrode prints on flexible base and the real image of manufactured wearable Silicon Carbide nanowire-network/tangle prototypes are shown in the (see Figure 3.5.a and 3.5.b). Moreover, a paste of Ag application on the edges of gold pads to probe and gather healthy data. The photograph of the flexible based Silicon Carbide NW-net UVPD for a single channel is taken under the optical microscopy (see Figure 3.5.c).

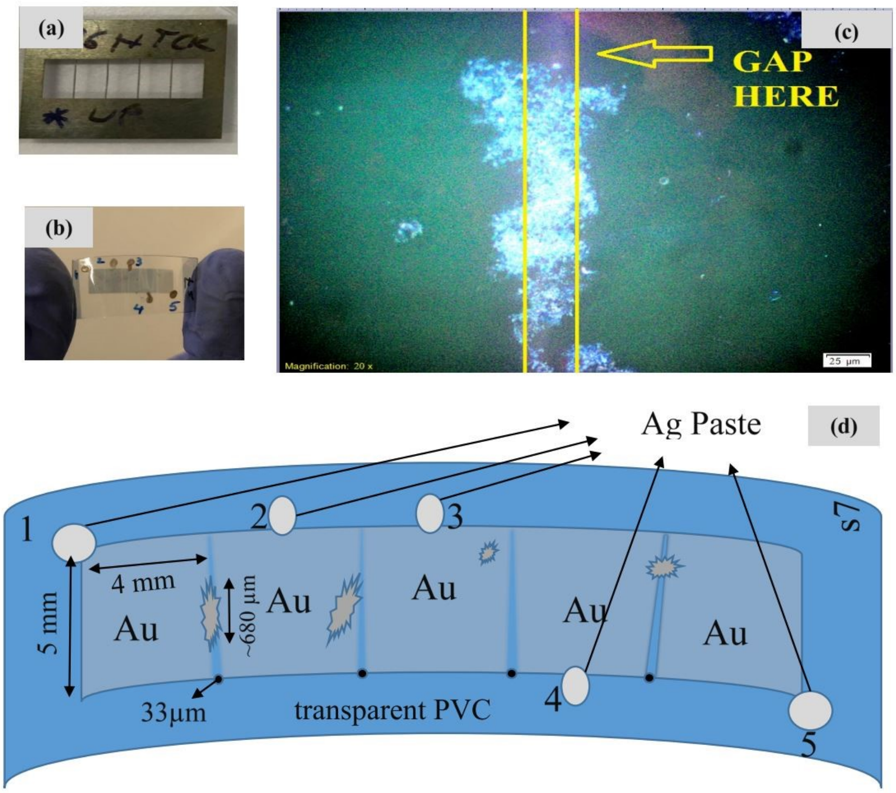

Figure 3.5: a) – The physical masks. b) – The final product. c) – The image of optical microscopy. d) – The Schematic drawing of the prototype manufactured.

The image taken under the optical microscope, obviously discloses the well fabricated working device NW-net between gold pads. The length of the nanowire network/tangle is just below 700 microns, and the width is slightly above 30 microns. The 2D scheme of the prototypes with critical distances are depicted in the (see Figure 3.5.d).

3.3. Comparison of Former Reports and This Work

Up until this point, a blind bit of works on theories and experiments are reported to optoelectronic characteristics of Silicon Carbide NW-forms. Table 1 facilitates to comprehend an all-inclusive comparative brief including contrasts, based on the indicators of material form, bias voltages, gap width, and reveals the KPIs (S, t_{rise}, t_{decay}, and R) of the devices of this work and some formerly investigated devices (see Figure 3.6).

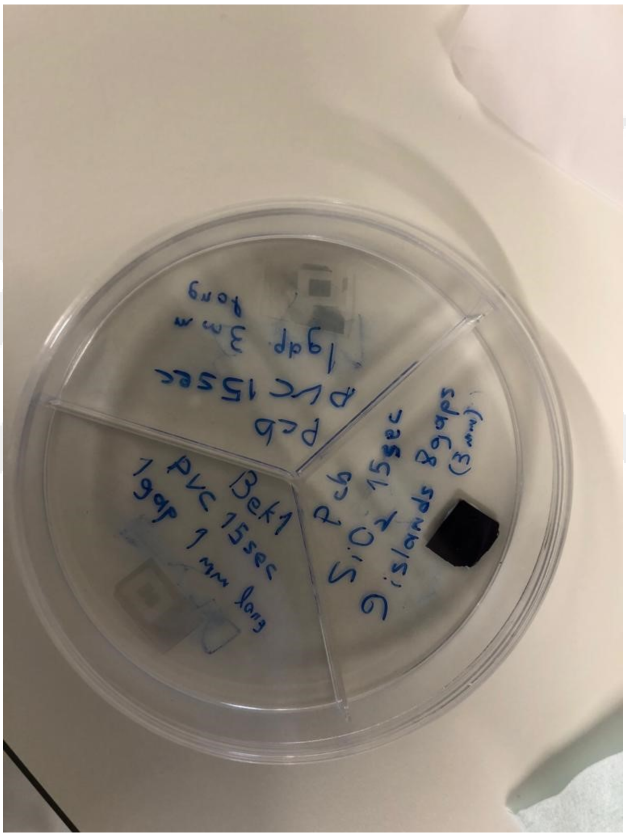

Figure 3.6: The UVPD prototype on two flexible based and one rigid wafer based devices of this dissertation, application of mask trials from the subcontractors.

Responsivity of this work's self-powered Silicon Carbide NW network/tangle UV sensor has very good performance than similar one, made of RGO at 2 bias. [Wang et al., 2014] and Aluminum Nitride nanowire network/tangle UV sensor at 15 bias on a flexible base [Ali and Teker, 2019]. Furthermore, the Silicon Carbide nanowire network/tangle UV sensor has much satisfactory S(%) results comparing both the flexible and rigid substrates. It is also remarkable that the performance figures of the 10-times bent device are ameliorated the optoelectrical characteristics. The possible explanation of this could be the better contact quality since, the performance of UVPD after 50 and 75-times bent UVPD expectedly are inversely proportional to the number of bendings. Last but not least, reasons how the characteristics of tests vary is statistically important [Wadsworth et al., 1986], but it is not that much observed and understandable in such an industry of its infancy like nano-manufacturing of industrial electronics.

4. CONCLUDING REMARKS

The trends in scale-down for IC devices and rising popularity of wearable electronics are internationally desirable for research and development regarding innovative alternatives and even a small difference in the morphological or geometrical designation might lead to big differences in the characteristics of the innovations. These devices are desired to work much faster with less energy consumption. Nevertheless, the bottleneck is the top-down manufacturing, bottom-up synthesis, and the integrated additive manufacturing among the traditional mass production and novel nano manufacturing techniques.

4.1. Conclusion and Future Studies

Nowadays, one of the hope-giving, bright and investigated nominees are one dimensional nanowires. The optoelectronic characterization of tangle Silicon Carbide NW-network UVPDs that portrayed roughly identical electrical properties of bare Silicon, is reported in this Master Dissertation. The claim of this work was exploring the innovation management by wearing laboratory gloves with witnessing an actual research and development, approaching to the difficulties of the researchers by hands-on experiencing them to define the problems in this field much better as an industrial engineer as the pre-requisite for mathematical modelling and optimization. The concentration of the work became a real research example for nanofabricating a prototype, reporting the characteristics of the Silicon Carbide nanowire-tangle UVPD KPIs such that PDCR, t_{rise}, t_{decay}, S, R. An informative introduction regarding nanostructural materials and the photonic, optoelectrical, and detecting applications of them has been given in first section. In addition, the summary of previously studied reports on photocurrent characteristics of UVPDs made of the comparable forms of materials are compiled. The prototyping and production of UV photosensors are represented including synthesizing TF and NW as well as characterizing them in the second section. The Silicon Carbide optoelectrical characterization are unveiled from defining the KPIs, followed by DOE, to compared by former reports. KPIs are namely, PDCR, S, R, photocurrent vs. time (I – t), rise and recovery times in the third section. KPIs are computed on Excel, and then matched by previous reports. The relationship between the related substitute materials is tabulated as Table 1.

Nanowire tangle-based Silicon Carbide's one of the photonic applications, UVPD, are well fabricated as a prototype after a couple of trials using trial-and-error and DTM method. Rewarding photocurrent properties are reported in terms of costs for total production and energy consumption of the UVPD. Indeed, the self-powered UVPD draw a figure of 15 for PDCR with~5.9 $mAxW^{-1}$ at UVC, ƛ= 0.254 microns. Consequently, the light response rate of the UVPD was very promising with rise time of ~1.69 seconds and recovery times of ~2.24 seconds, accordingly even at 0 V. In addition to that UVPD prototype performed quite interesting, stable, and satisfactory results in repeated tests for the objectives of simulating harsh circumstances and forecasting the estimated product life. Additionally, there is a no-power operating level likelihood to the detection even in as poor signaling as pico-levels with highly efficient yielding. To conclude, the withstanding in these conditions makes the powerless Silicon Carbide nanowire-tangle based UV sensor on PVC up-and-coming nominees for nano-electronics, printed & foldable devices, wearable technologies, next generation optoelectrical appliances when considering features such that reduced-cost, better performing, and easily-scalability to mass production.

Although synthesis and characterization of the prototype flex-SiC nanowire-tangle based UV detectors are well produced first-time in this work, as far as the best knowledge, there is a likelihood margin to develop further. Human factor and rigor prevail for being careful about fabrication environments without clean room and the indication of the topics with the developments imply they are in take-off. Although DTM is recently developed during the assembly of UV sensors to by-pass the photolithography procedures for manufacturing of nanowire-tangle SiC, the more precision and accuracy of fabricating nanowire-tangle products would be developed by employing diverse assembling methods since Langmuir-Blodget. The impact of such III-V or IV-IV novel hybrids, compounds, and composites for flexible PVC would be examined as the nano-manufacturing of the SiC nanowire-tangle UV detector is ready-to-apply and adjust to different surfaces with additive manufacturing.

The upcoming study would be a final product passing through additive manufacturing end-to-end for completely comprehensive understanding of the impacts and improvements would be the potential. Even lower-cost and simpler mechanism would be possible for UV sensors by comprehending the characteristics of Silicon Carbide single-nanowire photodetector rather than nanowire-tangle form of the material. Nevertheless, single-nanowire based product fabrication requires time, rigor, patience, and sophisticated expertise as a future study and an advanced manufacturing.

REFERENCES

Aksoy B., Coskun S., Kucukyıldız S., Unalan H. E., (2012), "Transparent, highly flexible, all nanowire network germanium photodetectors", Nanotechnology 23 325202-325210.

Akter T., Kim W. S., (2012), "Reversibly Stretchable Transparent Conductive Coatings of Spray Deposited Silver Nanowires", ACS Applied Materials & Interfaces 4 1855-1859.

Aldalbahi A., Li E., Rivera M., Velazquez R., Altalhi T., Peng X., Feng P. X., (2016), "A new approach for fabrications of SiC based photodetectors", Sci. Rep. 6 23457

Alenezi M. R., Henley S. J., Silva S. R. P., (2015), "On-chip Fabrication of High Performance Nanostructured ZnO UV Detectors", Scientific Reports 5 8516.

Ali Y. A., Teker K., (2019), "Fabrication of Ultraviolet Photodetector with Aluminum Nitride Nanowire Networks via Direct Transfer Method", Microelectronic Engineering 211 26-28.

Alsultany F.H., Hassan Z., Ahmed N.M., (2016), "A high-sensitivity, fast-response, rapid-recovery UV photodetector fabricated based on catalyst-free growth of ZnO nanowire networks on glass substrate", Optical Materials 60, 30-37.

AlZoubi T., Qutaish H., Al-Shawwa E., Hamzawy S., (2018), Enhanced UV-light detection based on ZnO nanowires/graphene oxide hybrid using cost-effective low temperature hydrothermal process, Optical Materials 77 226-232.

Ates E. S., Kucukyildiz S., Unalan H. E., (2012), "Zinc Oxide Nanowire Photodetectors with Single-Walled Carbon Nanotube Thin-Film Electrodes", ACS Applied Materials & Interfaces 4 5142-5146.

Boruah, B. D., Mukherjee A., Sridhar S., Misra A., (2015), "Highly Dense ZnO Nanowires Grown on Graphene Foam for Ultraviolet Photodetection", ACS Appl. Mater. Interfaces 7(19) 10606–10611.

Demesa T., Morisota F., Legallais M., Calaisa A., Pernota E., Pignot-Paintranda I., Ternona C., Stamboulia V., (2019), "DNA grafting on silicon nanonets using an eco-friendly functionalization process based on epoxy silane", Materials Today: Proceedings 6 333–339.

Gedamu D., Paulowicz I., Kaps S., Lupan O., Wille S., Haidarschin G., Mishra Y. K., Adelung R., (2014), "Rapid Fabrication Technique for Interpenetrated ZnO Nanotetrapod Networks for Fast UV Sensors", Adv. Mater. 26 1541.

Grottrup J., Postica V., Smazna D., Hoppe M., Kaidas V., Mishra Y.K., Lupan O., Adelung R., (2017), "UV detection properties of hybrid ZnO tetrapod 3-D networks", Vacuum 146 492-500.

Hauger T. C., Al-Rafia S. M. I., Buriak J. M., (2013), "Rolling Silver Nanowire Electrodes: Simultaneously Addressing Adhesion, Roughness, and Conductivity", ACS Applied Materials & Interfaces 5 12663-12671.

Hu L.F., Yan J., Liao M.Y., Wu L., Fang X.S., (2011), "Ultrahigh External Quantum Efficiency from Thin SnO2 Nanowire Ultraviolet Photodetectors", Small 7 1012-1017.

Hung C. M., Phuong H. V., Duy N. V., Hoa N. D., Hieu N. V., (2018), "Comparative effects of synthesis parameters on the NO_2 gas-sensing performance of on-chip grown ZnO and Zn2SnO4 nanowire sensors", Journal of Alloys and Compounds 765 1237-1242.

Jiang J., Heck F., Hofmann D. M., Eickhoff M., (2017), "Synthesis of SnO2 Nanowires Using SnI_2 as Precursor and Their Application as High-Performance Self-Powered Ultraviolet Photodetectors", Physica Status Solidi B 255 1700426.

Jeong S., Kim M. W., Jo Y. R., Leem Y. C., Hong W. K., Kim, B. J., Park S. J., (2016), "High-performance photoresponsivity and electrical transport of laterally-grown ZnO/ZnS core/shell nanowires by the piezotronic and piezo-phototronic effect", Nano Energy 30 208-216.

Kiasari N. M., Soltanian S., Gholamkhass B., Servati P., (2014), "Sketching Functional, Ubiquitous ZnO Nano-sensors on Paper", RSC Advances 4 19663-19667.

Lee S., Jung S. W., Park S., Ahn J., Hong S. J., Yoo H. J., Lee M. H. Cho D. D., (2012), "Fabrication and Evaluation of Silicon Nanowire Photodetectors on Flexible Substrate for Retinal Prosthetic System, Sensors and Materials" 24(4) 205–220.

Li G., Song E., Huang G., Pan R., Guo Q., Ma F., Zhou B., Di Z., Mei Y., (2018), "Flexible Transient Phototransistors by Use of Wafer-Compatible Transferred Silicon Nanomembranes", Small 1802985.

Li L., Zhang Y., Fang X., Zhai T., Liao M., Sun X., Koide Y., Bandoa Y., Golberg D., (2011), "WO3 nanowires on carbon papers: electronic transport, improved ultraviolet-light photodetectors and excellent field emitters", Journal of Materials Chemistry 21 6525-6530.

Liang Y., Liang H., Xiao X., Hark S., (2012), "The epitaxial growth of ZnS nanowire arrays and their applications in UV-light detection", Journal of Materials Chemistry 22 1199-1205.

Lien W. C., (2013), "Harsh Environment Silicon Carbide UV Sensor and Junction Field-Effect Transistor", A dissertation submitted in partial satisfaction of the requirements for the degree of Doctor of Philosophy in Applied Science & Technology in the Graduate Division of the University of California, Berkeley 1-27.

Liu B., Wang Z. R., Dong Y., Zhu Y. G., Gong Y., Ran S. H., Liu Z., Xu J., Xie Z., Chen D. Shen G. Z., (2012), “ZnO-nanoparticle-assembled cloth for flexible photodetectors and recyclable photocatalysts”, J. Mater. Chem. 22, 9379.

Liu Z., Huang H., Liang B., Wang X., Wang Z., Chen D., Shen G., (2012), “Zn_2GeO_4 and $In_2Ge_2O_7$ nanowire mats based ultraviolet photodetectors on rigid and flexible substrates”, Optics Express 20 2982-2991.

Miller M. S., O’Kane J. C., Niec A., Carmichael R. S., Carmichael T. B., (2013), Silver Nanowire/Optical Adhesive Coatings as Transparent Electrodes for Flexible Electronics, ACS Applied Materials & Interfaces 5 10165-10172.

Molina-Mendoza A. J., Moya A., Frisenda R., Svatek S. A., Gant P., Gonzalez-Abad S., Antolin E., Agraït N., Rubio-Bollinger G., de Lara D. P., Vilatela J. J., Castellanos-Gomez A., (2016), “Highly responsive UV-photodetectors based on single electrospun TiO2 nanofibres”, J. Mater. Chem. C 4 10707–10714.

Onder, M. S., Teker, K. (2022). “Direct Transfer Manufacturing of Flexible Silicon Carbide Nanowire-Network Prototype Device”. In Nano Hybrids and Composites (37, 49–58). Trans Tech Publications, Ltd. https://doi.org/10.4028/p-d0o9il ISSN: 2297-3400

Onder, M. S., Teker, K. (2022). “Direct Transfer Manufacturing of Flexible Silicon Carbide Nanowire-Network Prototype Device”. In Nano Hybrids and Composites (37, 49–58). Trans Tech Publications, Ltd. https://doi.org/10.4028/v-83yzd5 ISBN-13 (softcover): 9783036401355 ISBN-13 (eBook): 9783036411354

Pu L., Abbas A. S., Maheshwari V., (2014), “Electrochemical Synthesis on Nanoparticle Chains to Couple Semiconducting Rods: Coulomb Blockade Modulation Using Photoexcitation”, Advanced Materials 26 6491-6496.

Qu Y., Wu Z., Ai M., Guo D., An Y., Yang H., Li L., Tang W., (2016), “Enhanced Ga_2O_3/SiC ultraviolet photodetector with graphene top electrodes”, J. Alloys Compd. 680 247-251.

Selman A.M. Hassan Z., (2015), “Highly sensitive fast-response UV photodiode fabricated from rutile TiO_2 nanorod array on silicon substrate,” Sens. Actuators A Phys. 221, 15-21.

Sepulveda-Mora1 S. B., Cloutier S. G., (2012), Figures of Merit for High-Performance Transparent Electrodes Using Dip-Coated Silver Nanowire Networks, Journal of Nanomaterials 286104.

Serre P., Mongillo M., Periwal P., Baron T., Ternon C., (2015), “Percolating silicon nanowire networks with highly reproducible electrical properties”, Nanotechnology 26 015201.

Shafique S., Yang S., Wang Y., Woldu Y. T., Cheng B., Ji P., (2019), “High-performance photodetector using urchin-like hollow spheres of vanadium pentoxide network device”, Sensors and Actuators A 296 38–44.

Sun B., Sun Y., Wang C., (2018), “Flexible Transparent and Free-Standing SiC Nanowires Fabric: Stretchable UV Absorber and Fast-Response UV-A Detector”, Small 14 1703391.

Teker K., (2014), “Gallium nitride nanowire devices and photoelectric properties”, Sensors and Actuators, A: Physical 216 142-146.

Teker K., (2016), “Photoresponse characteristics of silicon carbide nanowires”, Microelectronic Engineering 162 79-81.

Ternon C., Serre P., Lebrun J. M., Brouzet V., Legallais M., David S., Luciani T., Pascal C., Baron T., Missiaen J. M., (2015), “Low Temperature Processing to Form Oxidation Insensitive Electrical Contact at Silicon Nanowire/Nanowire Junctions”, Advanced Elecronic Materials 1 1500172.

Wadsworth, Jr H. M., Stephens K. S., Godfrey A. B., (1986), “Modern Methods for Quality Control and Improvement”, Wiley & Sons Inc. NY, USA.

Wang J., Yan C., Lin M. F., Tsukagoshi K., Lee P. S., (2014), “Solution-assembled nanowires for high performance flexible and transparent solar-blind photodetectors”, Journal of Materials Chemistry C 3 596-600.

Wang X., Tian W., Liao M., Bando Y., Golberg D., (2014), “Recent advances in solution-processed inorganic nanofilm photodetectors”, Chemical Society Reviews 43 1400-1422.

Wang Z., Wang H., Liu B., Qiu W., Zhang J., Ran S., Huang H., Xu J., Han H., Chen D., (2011), “Transferable and Flexible Nanorod-Assembled TiO2 Cloths for Dye-Sensitized Solar Cells, Photodetectors, and Photocatalysts”, ACS Nano 5 8412.

Weng W. Y., Hsueh T. J., Chang S. J., Wang S. B., Hsueh H. T., Huang G. J., (2011), “A High-Responsivity GaN Nanowire UV Photodetector”, IEEE J. Sel. Top. Quantum Electron. 17(4) 996–1001.

Wyatt-Moon G., Georgiadou D. G., Semple J., Anthopoulos T. D., (2017), “Deep Ultraviolet Copper(I) Thiocyanate (CuSCN) Photodetectors Based on Coplanar Nanogap Electrodes Fabricated via Adhesion Lithography”, ACS Applied Materials & Interfaces 9 41965-41972.

Xu Z., Wu C., Li F., Chen W., Guo T., Kim T. W., (2018), Triboelectric electronic-skin based on graphene quantum dots for application in self-powered, smart, artificial fingers, Nano Energy 49 274–282.

Yip S., Shen L., Ho J. C., (2019), “Recent advances in flexible photodetectors based on 1D nanostructures, Journal of Semiconductors” 40(111602) (2019) 11–13.

Zhang Q., Jie J., Diao S., Shao Z., Zhang Q., Wang L., Deng W., Hu W., Xia H., Yuan X., Lee S. T., (2015), “Solution-Processed Graphene Quantum Dot Deep-UV”. ACS Nano 9 1561−1570.

BIOGRAPHY

I graduated from Industrial Engineering as valedictorian and did a master 's degree focusing on nano-electronics related with nano-manufacturing of UV sensors (SOI) using CVD, sputter coater, SEM, without photolithography. It is extended due to COVID-19 but I graduate at the end of the 2021-22 spring semester. My research interest for the future relies on Electronics (NEMS, MEMS, MOEMS, ioNT). Beside my NEMS, and Nano-manufacturing courses taken in Master's, I had a hands-on lab experience around 2 years in Marmara University, I had a chance to visit UTT, Troyes as an exchange researcher in my master and take the chance of observing AFM in ONT and L2n Lab. Before and after my exchange, I had also experience as undergraduate TA (UGTA) 2.5years, Graduate TA experience 3 years, total of 5 to 6 years. Recently I have transferred to Gebze Technical University (former Gebze Institute of Technology) and have taken Linear Programming and Industrial Statistics courses, passed with A as my all-other Master courses. Moreover, I have been accepted to the Advanced Nano Materials (ANM) 2022 conference on 27th of April,2022 and presented on 27th of July,2022.

APPENDICES

Appendix A: Publications

Onder, M. S., Demiriz, A., Teker, K. (2022). "Powerless Flexible Silicon Carbide Nanowire-Nanowire Junction Ultraviolet Photodetector via Direct Transfer Method", 19th International Conference on Advanced Nano Materials, Aveiro, Portugal, 27-29 July.

Onder, M. S., & Teker, K. (2022). "Direct Transfer Manufacturing of Flexible Silicon Carbide Nanowire-Network Prototype Device". In Nano Hybrids and Composites (37, 49–58). Trans Tech Publications, Ltd. https://doi.org/10.4028/p-d0o9il ISSN: 2297-3400

Onder, M. S., & Teker, K. (2022). "Direct Transfer Manufacturing of Flexible Silicon Carbide Nanowire-Network Prototype Device". In Nano Hybrids and Composites (37, 49–58). Trans Tech Publications, Ltd. https://doi.org/10.4028/v-83yzd5 ISBN-13 (softcover): 9783036401355 ISBN-13 (eBook): 9783036411354

Appendix B: Additional Figures

I-V Characteristics–Fig.4

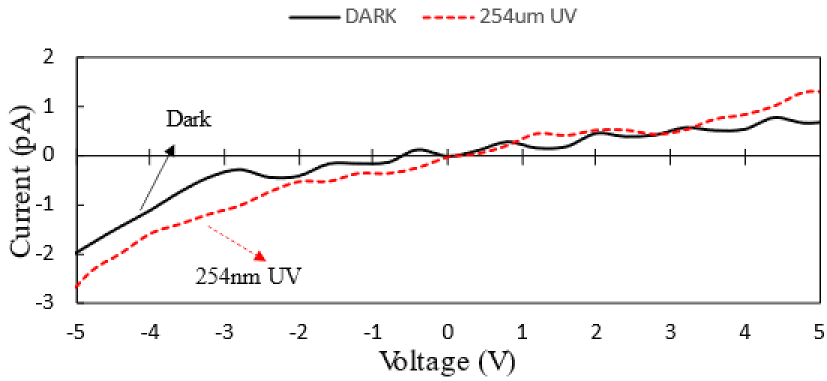

Figure 4. *I vs. V* photocurrent properties of the 3C-SiC UV photosensor in dark and under 254 nm wavelength ultraviolet light.

Rise and Decay –Fig.eski7

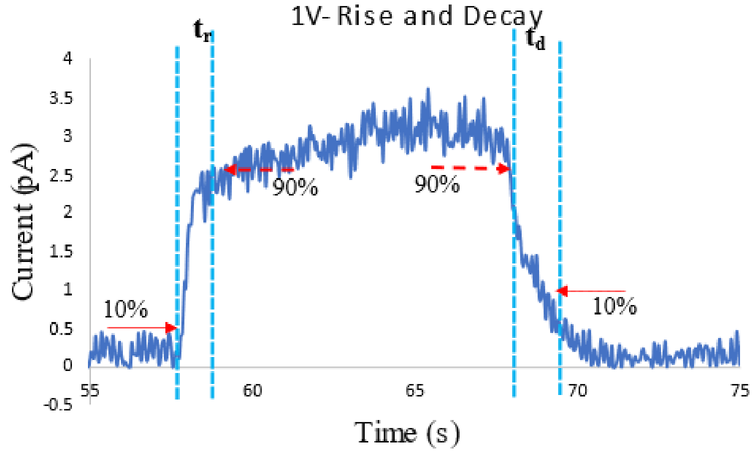

Figure ~~x~~7. The rise and decay times are 1.95 s and 1.65 s, respectively calculated by t90= 59.77substracted from t10=57.82 and t' 10= 69.45 substracted from t' 90= 67.8 at room temperature and a bias voltage of 1 V.

Sensitivity vs Voltage – Fig.eski 8

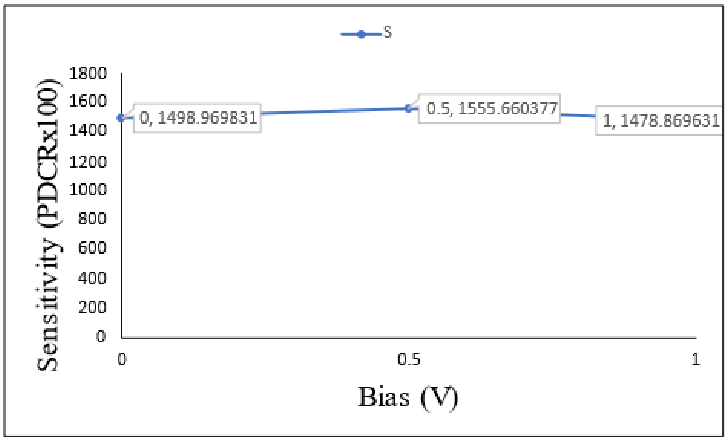

Figure x8. The sensitivity (S) of the 3C-SiCNW-UVPD for the biases differing at 0 V, 0.5 V and 1 V voltages.

RiseDecay and Responsivity– Fig.8

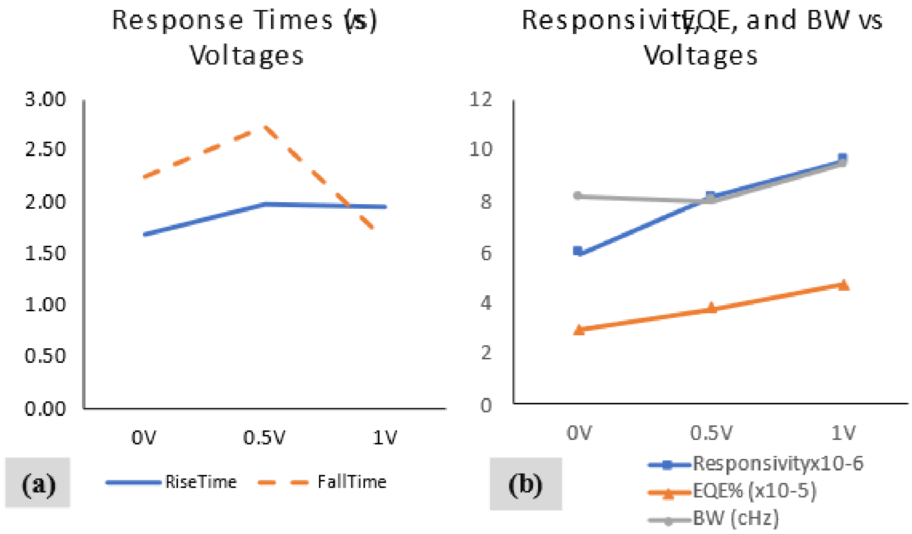

Figure 8. (a) The rise and decay time illustrations in different biases **(b)** The responsivity EQE and BW demonstrations in varying biases at low voltages. EQE and BW are going to be calculated and edited/added here. The EQE and BW now is only makeup nonsense no.

Bending Comparison – Table 2.

Table 2. Bending results comparisons of Silicon Carbide Nanowire based UV photodetectors at four different bending cycle amount, namely 0, 10, 50, 75 at 1 V.

Current (pA)	BeforeBending	10Bending	50Bending	75 Bending
Ion	~0.6	~1.3	~1.1	~0.5
Ioff	~0.2	~0.49	~0.39	~0.19